

Photoactive Titania and Nanoparticulate Silver-Titania Composite Thin Films as Potent Antimicrobial Coatings

K. Page*, I. P. Parkin* and M. Wilson**

*Department of Chemistry, University College London, 20 Gordon Street, London, WC1H 0AJ, UK. kristopher.page@ucl.ac.uk and i.p.parkin@ucl.ac.uk

**Division of Microbial Diseases, UCL Eastman Dental Institute, University College London, 256 Gray's Inn Road, London, WC1X 8LD, UK. m.wilson@eastman.ucl.ac.uk

ABSTRACT

Titania (anatase) and Ag-doped titania (anatase) coatings were prepared on glass microscope slides by sol-gel dip-coating. Coatings were characterised by XRD, XANES, SEM/WDX, XPS and UV visible techniques and consisted of anatase with ca 1 - 0.2 atom % Ag₂O. Photocatalytic activity of the coatings was determined by photomineralisation of stearic acid, monitored by FT-IR. Active coatings were screened for their antibacterial efficacy against *Staphylococcus aureus* (NCTC 6571), *Escherichia coli* (NCTC 10418) and *Bacillus cereus* (CH70-2). Ag-doped titania coatings were significantly more active than a titania coating. No antimicrobial activity was observed in the dark – indicating that silver ion diffusion was not the mechanism for antimicrobial action. The mode of action was explained in terms of a charge separation model. The Ag₂O/TiO₂ coating is a potentially useful coating due to its robustness, stability to cleaning/reuse, and its antimicrobial response.

Keywords: titania photocatalysts, antimicrobials

1 INTRODUCTION

Since the discovery of the photolysis of water by a TiO₂ photochemical cell [1] and the subsequent demonstration of photocatalytic disinfection of microbial cells [2], research into photoactive nanocomposite thin films as antimicrobial surfaces has become widespread. This is of particular importance in light of recent growing concerns regarding nosocomial infections, such as MRSA, in UK hospitals. Surface contamination by microorganisms such as MRSA is clearly implicated in the transmission of nosocomial pathogens [3-6] and hence self disinfecting surface treatments, based on TiO₂ photocatalysts are of great scientific and commercial interest. This research focuses on the study of nanocomposite titania thin films and their application as antimicrobial surfaces [7].

2 EXPERIMENTAL

All materials were prepared in air by a simple sol-gel method, relying upon a condensation polymerisation type

reaction. Coatings were deposited onto standard low iron microscope slides by a dip coating technique.

2.1 Sol-gel Synthesis

Titanium n-butoxide (17.02 g, 0.05 mol) was added to a mixture of pentane-2,4-dione (2.503 g, 0.025 mol) in butan-1-ol (32 cm³, 0.35 mol) to chelate the titanium precursor. A clear, straw yellow solution was produced, with no precipitate. This solution was covered with a watch glass and stirred for an hour. Distilled water (3.6 g, 0.2 mol) was dissolved in propan-2-ol (9.04 g, 0.15 mol) and added to the stirring solution to hydrolyse the titanium precursor. The solution remained a clear straw yellow colour, with no precipitate. The solution was stirred for a further hour. Silver nitrate (0.8510 g, 0.005 mol) was dissolved in acetonitrile (1.645 g, 0.04 mol). This was added to the pale yellow titanium solution, which was stirred for a final hour. After the final stirring, the resultant sol was a slightly deeper yellow in colour, but remained clear and without precipitate. The sol was used within 30 minutes for dip-coating. The TiO₂ film controls were made in a similar manner by excluding the addition of the AgNO₃. TiO₂ controls were made to the same thickness/crystallinity as the Ag doped samples.

2.2 Film Deposition by Dip Coating

All coatings were deposited onto standard low iron microscope slides (BDH/VWR UK) by a sol-gel dip coating method. The sol was stirred and transferred to a tall form 50 cm³ beaker. This enables the majority of the slide to be coated. A custom dip-coating apparatus was used to withdraw the slide from the sol at a rate of 120 cm min⁻¹. Multiple coats were deposited by re-dipping the slide after allowing the previous coat to air dry. Deposited coatings were then annealed at 500 °C for one hour to produce a crystalline coating.

3 SAMPLE CHARACTERISATION

Samples were characterised using a variety of techniques, including field emission SEM, wavelength dispersive X-

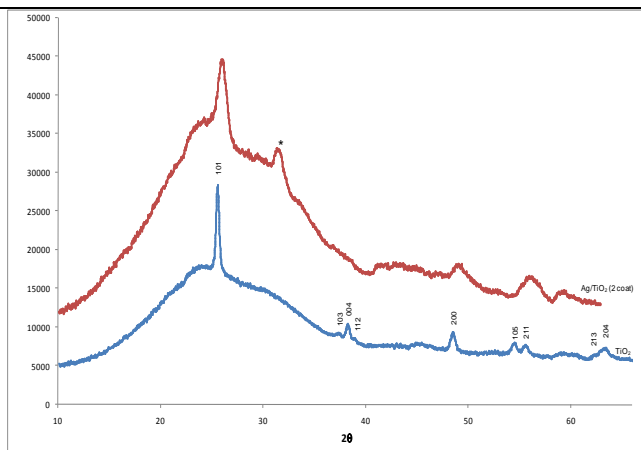


Figure 1 Powder XRD patterns for four coat TiO₂ (lower trace) and two coat Ag-TiO₂ coatings (upper trace). The Ag-oxide peak is marked with an asterisk (*).

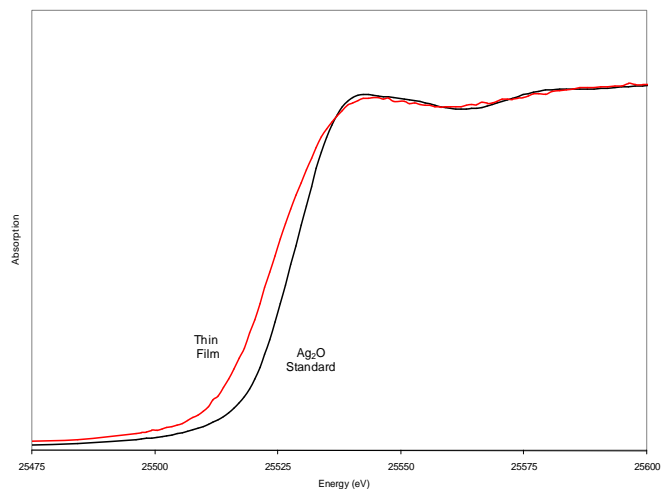


Figure 2 The Ag K-edge XANES for Ag₂O and Ag-doped TiO₂ film

ray analysis, powder XRD and XAS (XANES) measurements. Functional properties of the coatings were also examined. The photocatalytic ability of the films was assessed by monitoring the photodegradation of stearic acid via FTIR. Photoinduced superhydrophilicity was examined by measuring the contact angle of a droplet of water placed onto the coating surface. Microbicidal activity was assessed with *Staphylococcus aureus* (NCTC 6571), *Escherichia coli* (NCTC 10418) and *Bacillus cereus* (CH70-2; mixed vegetative and endospore). Microbiology experiments were performed in duplicate and repeated at least twice.

4 RESULTS

4.1 Physical Characterisation

Deposited films were well adhered to the glass substrate and could not be removed by peeling off Scotch® tape. The films were also resistant to scratching with a stainless steel spatula edge. The film was only removed by chipping at the glass substrate or by scratching with a diamond tipped stylus. Repeated dips of a coated substrate into distilled water had no effect on the adherence of the coating. The films had a multicoloured hue due to refringence effects resulting from variation in the coating thickness. The Ag doped films had a distinct bluish hue, which was not apparent in the TiO₂ controls. The stability of the coatings is akin to those deposited by CVD [8, 9], rather than traditional sol-gel and paste [10, 11] methods.

4.2 Characterisation

Powder X-Ray diffractograms of the TiO₂ films were indexed as anatase ($I4_1/amd_z$, $a = 3.776 \text{ \AA}$, $c = 9.486 \text{ \AA}$). The Ag/TiO₂ diffractograms were slightly less well

defined than the TiO₂ diffractogram but did show peaks attributed to anatase TiO₂ (Figure 1). Furthermore, the Ag/TiO₂ patterns exhibited one other significant peak at 31.5° 2θ which was absent in the TiO₂ pattern and must therefore be due to the difference in composition – possibly due to the incorporation of a Ag compound rather than crystalline Ag. Database patterns for crystalline Ag do not correlate with this observed peak. The best pattern match for this peak and the remainder of the diffractogram is for the silver oxides AgO and Ag₂O. Both silver oxide species correspond well with their most intense peaks aligning with the additional peak observed in the experimental pattern.

Extended X-Ray Fine Structure XANES measurements (Figure 2) and XPS spectra, along with WDX analysis showed the Ag to be present in the form of the silver oxide Ag₂O. These techniques characterised the samples as anatase TiO₂ with 0.2-1 atom% Ag₂O. UV visible spectroscopy showed a characteristic anatase band edge at approximately 380 nm and band gap extrapolation plots yielded optical band gaps in the region of 3.0 eV. Anatase TiO₂ has a band gap energy of 3.2 eV. [12]

SEM was used to study the morphology of the coated surfaces. SEM imaging showed minor shrink cracking in the single or double dip-coated films. The severity of shrink cracking increased with increasing film thickness. At higher magnifications, both coating types had similar morphologies, consisting of granular structures. The nanocrystalline nature of the TiO₂ materials was observed – particles of 30 nm size on average can be seen in a x200000 image (Figure 3). Observation of particles of this size correlates well with the crystallite sizes calculated by the Scherrer equation from the XRD line broadening – which corresponds best to nanocrystalline titania, rather than a fully crystalline phase. End on SEM

studies were also carried out to measure the thickness of the films. The two coat materials had a thickness of approximately 150 nm and a four coat material was approximately twice this thickness, at ca. 300 nm.

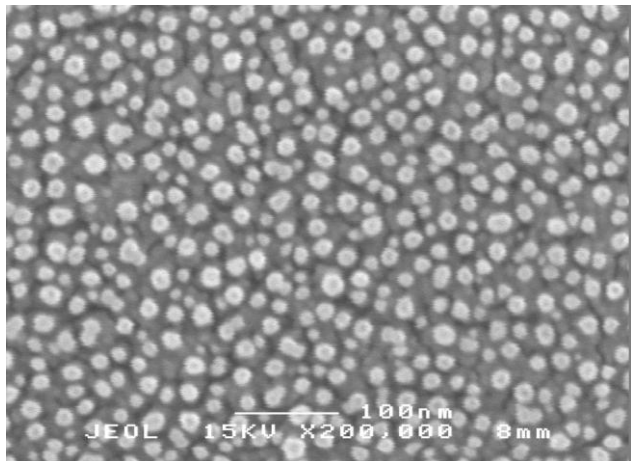


Figure 3 SEM image of TiO₂ coating x200,000, scale bar 100 nm

4.3 Functional Properties

4.3.1 Photocatalysis and water droplet contact angle

All of the samples demonstrated photocatalytic activity against an overlayer of stearic acid when illuminated by 254 nm germicidal UV lamp. Ag doped materials were significantly more photoactive than a corresponding TiO₂ control. Photocatalytically active films were hydrophilic as made (ca. 15°) and also demonstrated photoinduced superhydrophilicity upon UV illumination with contact angles reducing to ca. 1° after illumination.

4.3.2 Antimicrobial Activity

The antimicrobial activity of the coatings was assessed against 3 different micro-organisms; *Staphylococcus aureus* (NCTC 6571), *Escherichia coli* (NCTC 10418) and *Bacillus cereus* (CH70-2). *S. aureus* is of interest because of its association with MRSA hospital acquired infections. *S. aureus* is also a typical Gram-positive organism, so it serves as a useful indicator of the behaviour of a sample coating towards this class of micro-organism. *E. coli*, was used as an example of a Gram-negative organism and *B. cereus*, as an example of a Gram-positive organism which forms spores under adverse conditions. The same coatings were reused for all antimicrobial testing and all experiments were carried out in duplicate and repeated twice. The samples were cleaned between uses by wiping with isopropanol wipes (as commonly used to clean hard surfaces in hospitals). The Ag-doped coatings performed very well under

conditions of reuse, maintaining a constant level of effectiveness despite being handled, cleaned and reused.

Staphylococcus aureus (NCTC 6571)

Experiments with *S. aureus* were carried out on timescales of two, four hours and six hours. Both undoped titania and the Ag-doped TiO₂ coatings displayed antibacterial activity towards *S. aureus*, although to varying degrees (Figure 4). The two-coat Ag/TiO₂ coating proved to be extremely effective against *S. aureus*. After six hours of illumination under 365 nm UV radiation the two coat Ag/TiO₂ coating was 99.997% effective against an inoculum of approximately 2.15 x 10⁹ cfu/ml *S. aureus*. As a point of reference, the analogous TiO₂ coating displayed an effectiveness of 49.925% against the same inoculum. Additional experiments were carried out with shorter illumination times (two and four hours). These experiments demonstrated a typical dose response profile relating the UV dose to the antimicrobial potency. It also enabled comparison of coating types and their efficacy – showing the two coat Ag-doped material to be a superior antimicrobial than the control.

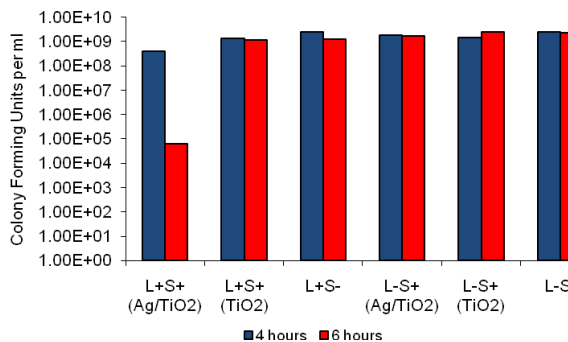


Figure 4 Bacterial kills for the two coat Ag/TiO₂ sol-gel prepared coating against *Staphylococcus aureus* after 4 and 6 hour illumination times with 365 nm radiation. The viable counts are expressed as colony-forming units/ml. L+S+ refers to the exposure of an active coating (identity in brackets) to UV light. L+S- refers to the exposure of an uncoated slide to UV light. L-S+ refers to an active coating (identity in brackets) kept in the dark and L-S- refers to an uncoated slide kept in the dark.

Escherichia coli (NCTC 10418)

Antimicrobial potency against *E. coli* was assessed in a six hour experiment using the two coat Ag-doped material only. Antimicrobial efficacy was not as striking as with *S. aureus*, but the coatings still exerted an antimicrobial effect. The coating averaged an effectiveness of 69% against an inoculum of ca. 2.61 x 10⁹ cfu/ml *E. coli*. The coating is noticeably less effective against *E. coli* than *S. aureus*, even though the size of the inoculum was similar.

Bacillus cereus (CH70-2)

The two-coat Ag/TiO₂ coating was also tested against *B. cereus*, another Gram-positive organism, but one that forms spores under adverse environmental conditions. Four and two hour experiments were carried out against this organism using the two coat Ag/TiO₂ coating only. The coating achieved greater than 99.9% kills of this organism at both 2h and 4h exposure periods with 365 nm UV. The inoculum in these experiments was lower than that used in other experiments, with a *B. cereus* initial concentration of ca. 1.0 x 10⁸ cfu/ml. Further, the UV light control L+S- showed no measurable kill at 2 hours and a 64% kill at 4 hours of exposure. This demonstrates that the coating is extremely effective after just 2 hours against an inoculum in the region of one hundred million cfu/ml. This level of contamination is still significantly greater than what would be found on a contaminated surface. For example, *S. aureus* contamination of a surface was shown typically to be between 4 and 7 cfu/cm². [13]

5. CONCLUSION

Photocatalytically-active and antimicrobially-active coatings were synthesised by a simple sol-gel dip coating technique. The resultant coatings were characterised by glancing angle X-ray diffraction, XPS, XANES, SEM/WDX and UV visible spectroscopy and shown to consist of anatase titania with embedded Ag₂O particles. Photocatalytic activity of the coatings was determined by photomineralisation of stearic acid and monitored by FT-IR spectroscopy. Coatings demonstrating high photocatalytic activity against stearic acid were then screened for antibacterial efficacy against *Staphylococcus aureus* (NCTC 6571), *Escherichia coli* (NCTC 10418) and *Bacillus cereus* (CH70-2). Ag-doped coatings were found to be significantly more photocatalytically and antimicrobially active than a regular TiO₂ coating. This can be explained in terms of a charge separation model. It is suggested that the silver species act as a source of electrons and as charge separators because of their high electron density relative to the TiO₂ matrix. These factors would enhance the overall photoactivity of the coating by firstly donating extra electrons to the conduction band which in turn are able to produce more reactive species at the catalyst surface, and secondly by blocking electron-hole recombination which stops the production of the reactive radicals at the surface.

Notably the coatings showed no activity against bacteria in the dark – indicating that their efficacy is not due to diffusible silver ions acting as a microbicide. The coatings also demonstrated significantly higher activity against the Gram-positive organisms than against the Gram-negative. This can be explained in terms of the comparative morphologies of the cell envelopes and the permeability of these envelopes to the likely toxic agent, the hydroxyl

radical. The morphology of the Gram-negative envelope affords greater protection against hydroxyl radicals because of the presence of two cell membranes. The Gram-positive envelope has only one membrane – which once breached by the reactive radicals results in cell death due to leakage of intracellular components.

The two coat Ag/TiO₂ coating would appear to be a potentially useful coating for hard surfaces in a hospital environment due to its robustness, stability to cleaning and reuse, and its excellent antimicrobial response to all organisms tested thus far. Such a coating would need to be applied at the point of manufacture of a particular item – and could not be retrofitted to existing surfaces because of the heat treatment required to generate the active coatings. However on new products it could create a very potent antimicrobial coating.

REFERENCES

1. A. Fujishima and K. Honda, *Nature*, **238**: p. 37-38, 1972.
2. T. Matsunaga, R. Tomoda, T. Nakajima, and H. Wake, *FEMS Microbiology Letters*, **29**(1-2): p. 211-214, 1985.
3. S.J. Dancer, *Journal of Hospital Infection*, **56**(1): p. 10-15, 2004.
4. B. Hota, *Clinical Infectious Diseases*, **39**(8): p. 1182-1189, 2004.
5. J.M. Boyce, G. Potter-Bynoe, C. Chenevert, and T. King, *Infection Control and Hospital Epidemiology*, **18**(9): p. 622-627, 1997.
6. D. Talon, *Journal of Hospital Infection*, **43**(1): p. 13-17, 1999.
7. K. Page, R. Palgrave, I.P. Parkin, M. Wilson, S.L.P. Savin, and A.V. Chadwick, *J. Mater. Chem.*, **17**: p. 95-104, 2007.
8. H.M. Yates, M.G. Nolan, D.W. Sheel, and M.E. Pemble, *Journal of Photochemistry and Photobiology A: Chemistry*, **179**: p. 213-223, 2006.
9. A.C. Jones, T.J. Leedham, P.J. Wright, M.J. Crosbie, K.A. Fleeting, D.J. Otway, P. O'Brien, and M.E. Pemble, *J. Mater. Chem.*, **8**(8): p. 1773-1777, 1998.
10. B.F. Xin, L.Q. Jing, Z.Y. Ren, J.Q. Wang, H.T. Yu, and H.G. Fu, *Acta Chimica Sinica*, **26**: p. 1110, 2004.
11. X.F. You, F. Chen, J.L. Zhang, J.S. Huang, and L.Z. Zhang, *Chinese Journal of Catalysis*, **27**: p. 270, 2006.
12. A. Mills and S. LeHunte, *Journal of Photochemistry and Photobiology a-Chemistry*, **108**(1): p. 1-35, 1997.
13. W.A. Rutala, E.B.S. Katz, R.J. Sherertz, and F.A. Sarubbi, *Journal of Clinical Microbiology*, **18**(3): p. 683-688, 1983.